STRUCTURE AND PHYSICAL PROPERTIES OF Pb–Sn MELTS

V. SKLYARCHUK,[1] A. YAKYMOVYCH,[1] I. SHTABLAVYY,[1]
I. SHEVERNOHA,[1] M. KOZLOVSKII,[2] R. KHAIRULIN,[3] S. STANKUS[3]

[1]**I. Franko L'viv National University, Chair of Metal Physics**
(8, Kyryla i Mefodiya Str., L'viv 79005, Ukraine; e-mail: `vasylsklyarchuk@gmail.com`*)*

[2]**Institute of Condensed Matter Physics, Nat. Acad. of Sci. of Ukraine**
(1, Sventsits'kogo Str., L'viv 79011, Ukraine; e-mail: `mpk@icmp.lviv.ua`*)*

[3]**S.S. Kutateladze Institute of Heat Physics of the RAS**
(1, Academician Lavrent'ev Prosp., Novosibirsk 630090, Russia; e-mail: `stankus@itp.nsc.ru`*)*

PACS 61.25.Mv

We study the structure, mutual diffusion, electrical resistance, thermopower, and viscosity of Pb–Sn melts in a wide temperature interval. On the basis of revealed differences between the curves of heating and cooling for the temperature dependences of electrophysical and structure-sensitive properties, as well as the hysteresis observed in the heating-cooling cycles, we assume the existence of a metastable microheterogeneous structure in Pb–Sn melts in a certain temperature interval.

1. Introduction

Numerous studies of the melts of eutectic and near-eutectic systems revealed a contradictory ambiguous behavior of many physical properties [1, 2]. A part of studies and the subsequent interpretation of results were based on the model of statistical distribution of atoms in melts, whereas some researchers used the quasieutectic model which is not identified with the crystal eutetic but is considered in a dynamical sense [1]. We note that, from the structural point of view, the notion of quasieutectic does not contradict the modern ideas of the fluctuation origin of concentration inhomogeneities. Eutectic melts can be considered as the alteration of microregions with fuzzy edges, and the atomic concentration of these regions is close to that of solid solutions composing the eutectic. At the same time, the continuous mass exchange between these microregions occurs. As a result of different approaches to the interpretation of diffractometric data, the direct structural studies give no unambiguous answer to the question about a microinhomogeneous structure of eutectic melts. The quantitative estimation of these results allows one to consider that the melts can be characterized by both quasieutectic or statistical and intermediate distributions of atoms. The more complete information about a structural inhomogeneity can be obtained from studies of electrophysical and structure-sensitive properties.

Lead-tin alloys are widely used in advanced technologies due to their unique properties such as the high plasticity, low melting temperature, and suitable wettability and electrical resistance [2]. However, certain limitations are met in practical applications. They are related, for example, to the deformational strengthening or the excessive growth in intermetallidic phases on the surface of solder-substrate joints [3–5]. Studies of the Pb-Sn eutectic by the method of absorption of gamma-rays revealed some anomalies on density polytherms which were explained by the transition of a melt structure from the quasieutectic state to a microhomogeneous one [6, 7]. According to new data on the density and the results of diffraction studies, the irreversible structural changes which occur in the eutectic melt of Pb-Sn depend on the temperature [8]. Moreover, with regard for the distinctions between the curves of heating and cooling for various characteristics of other similar eutectics [9], the more profound studies of Pb-Sn melts seem actual. Pb-Sn alloys are also frequently used as model objects in studies of the crystallization [10, 11], and the information about the temperature dependences of their physical properties is urgent for a numerical modeling. Here, we present the results of studies of the mutual diffusion, electrical conduction, thermopower, and viscosity of Pb-Sn melts in a wide temperature interval, by accentuating the specific features of behavior of these properties at the melting and the crystallization.

2. Experimental

2.1. Studying the structure

Studying the structure was carried out with the help of a high-temperature X-ray diffractometer allowing the determination of the diffracted emission at various temperatures up to 1600 K. A specimen was positioned in the chamber of a diffractometer filled by helium. The geometries of positions of the input slit for X-rays made monochromatic with the help of a LiF crystal, chamber center, and input slit of a counter corresponded to a focusing scheme of the Bragg–Brentano type. The measurement error of the emission intensity amounted to 2–3% and depended on the chosen exposition duration of at each point. The temperature was measured to within ±2 K. The obtained experimental angular dependences of the diffracted emission were averaged with the use of the method of least squares. Then we corrected them with regard for the polarization, absorption, and anomalous dispersion [12]. The normalized curves of the intensity were used for the calculation of the structural factors, binary correlation functions, and distribution functions of the atomic density which allow us to determine the coordination numbers Z.

2.2. Study of the mutual diffusion

We used the experimental procedure based on the periodic scanning of an inhomogeneous melt by a narrow beam of hard gamma-quanta and the determined dependences of the emission attenuation coefficient of a specimen on the time and the coordinate (height). These measurements allow one to determine the time evolution of profiles of the concentration and the density in the process of diffusion mass transfer. Using the data on the relaxation of the density at a long-term holding duration, we calculated the coefficients of mutual diffusion $D(T)$. The calculation was based on the well-known asymptotic solutions of the equations of nonstationary diffusion with relevant boundary and initial conditions. In fact, the method is an analog of capillary methods to investigate the mutual diffusion which are widely used in a study of high-temperature melts. However, as distinct from the mentioned methods, the distribution of components is determined in our case directly in a liquid specimen. Respectively, the factors such as a concentration profile distortion at the crystallization of a melt due to liquation phenomena and the shrinkage (the main sources of errors of the capillary methods) do not affect the accuracy of measurements. High-temperature experiments were carried out in the atmosphere of pure argon. The crucibles for melts were produced of stainless steel. The temperature was measured by chromel-alumel thermocouples, whose calibration was verified by the melting points of Pb and Sn. The error of measurements of the temperature was at most 0.5 K. A detailed description of the experimental setup, procedure of measurements, and treatment of results is given in [13]. The error of the determination of the coefficients of mutual diffusion which depend on both the absolute value of D and the initial drops of the concentration in specimens is in the limits 8–20%.

2.3. Study of electrical resistance and thermopower

The measurements were carried out in argon at a pressure of at most 10 MPa by the contact method by a 4-point scheme. We used measuring cells made of pressed boron nitride in the form of vertical containers 60 mm in height and 3 mm in diameter. The cell structure allows one to simultaneously measure the electrical resistance and the thermopower. A high-temperature heater with three independently controlled heating elements held a uniform temperature field in the limits of 0.2–0.3 K in a working temperature interval at measurements of the electrical resistance or created the temperature gradient up to 15–20 K along a cell at measurements of the thermopower. Lead and tin weighed to within 10^{-4}g (CHEMPUR, Feinchemikalien und Forschungsbedarf GmbH, 99.999%) were synthesized in evacuated and soldered quartz ampoules at a residual pressure of 10—15 Pa and then sealed directly into a cell. The experimental setup and the procedure of measurements are described in [14]. The errors of determination of the electrical resistance, $\rho(T)$, and the thermopower, $S(T)$, do not exceed, respectively, 2% and 5%.

2.4. Study of the heat conduction

The heat conduction was studied by the stationary method of coaxial cylinders [15]. The measuring cells were fabricated of BN. An internal heater created a necessary temperature gradient in a melt. An external three-section heater allowed us to regulate the temperature field over height. For the control over the temperature, we used tungsten-rhenium thermocouples WR5/20. Two thermocouples were placed in the internal cylinder and controlled a distribution of the temperature over the heater radius. The coefficient of heat conduction, $\lambda(T)$, was calculated by the well-known formula for the heat transfer in a cylindrical layer

$$\lambda = \frac{Q \ln(d_2/d_1)}{2\pi l (T_1 - T_2)}, \tag{1}$$

where Q is the amount of heat released by a heater per unit time, and d_1 and d_2 are the external diameter of the

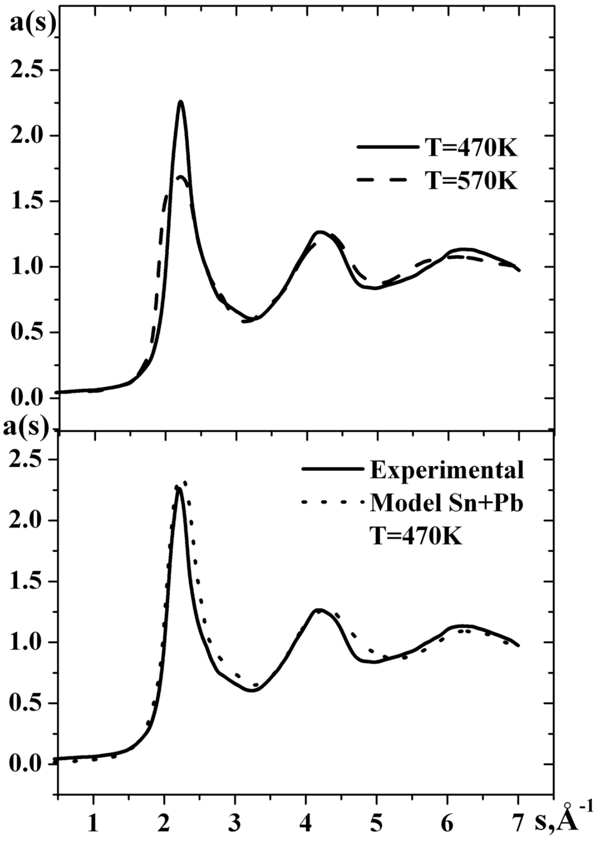

Fig. 1. Structural factors of the liquid eutectic $Pb_{26}Sn_{74}$

internal cylinder and the internal diameter of the external cylinder, respectively. The setup structure ensured the minimum heat loss and the minimum convection. The error of determination of the heat conduction was at most 7%.

2.5. Study of the viscosity

Measurements of the viscosity were carried out on a computerized viscosimeter with rotatable crucible [16]. Measuring cells were fabricated of graphite in the form of a cylindrical container with the internal diameter of 14 mm and the height of 30 mm. The period and the logarithmic damping decrement of oscillations were determined with the help of an optical system. The viscosity was calculated by the Roscoe's modified equation for specimens of cylindrical shape with open surface [17]. Measurements were performed in the atmosphere of 90 % Ar + 10 % H_2. In the chamber, we held a homogeneous temperature field to within 0.5 K in a range up to 800 K. The temperature was measured with the help of a WRe-5/20 thermocouple placed under a container. The error of measurements of the viscosity was at most 3 %.

3. Results

The structural factors for the liquid eutectic $Pb_{26}Sn_{74}$ are obtained at temperatures of 470 K и 570 K (Fig. 1). As seen from the figure, a specific feature of the structural factor of the eutectic $Pb_{26}Sn_{74}$ at a temperature of 470 K is a secondary maximum, like that in pure tin. This fact testifies to the presence of groups of atoms with the covalent type of coupling in the eutectic melt. As the temperature increases by 100 K, the asymmetry of the right branch of the structural factor decreases. The position of the first maximum of the eutectic at $T = 470$ K ($s_1 = 2.21$ Å^{-1}) is between those for pure tin ($s_1 = 2.20$ Å^{-1}) and lead ($s_1 = 2.27$ Å^{-1}). The same behavior is also characteristic of the height of the principal maxima ($a_{\mathrm{Pb}_{26}\mathrm{Sn}_{74}} = 2.36$, $a_{\mathrm{Sn}} = 2.28$, $a_{\mathrm{Pb}} = 2.48$). As the temperature increases, the height of the first maximum of the structural factor for the melt of $Pb_{26}Sn_{74}$ decreases, whereas the width increases, which indicates a decrease in the mean atomic density of the melt. By using binary correlation functions, we found that the mean interatomic distances increase with increase in the temperature by 100 K ($R_1 = 3.30$ Å at $T = 470$ K, and $R_1 = 3.34$ Å at $T = 570$ K). The same behavior is also characteristic of the mean coordination number ($Z = 8.3$ at $T = 470$ K, and $Z = 9.0$ at $T = 570$ K).

The results of measurements of the mutual diffusion are given in Fig. 2. We present also the results of our previous studies of the melt of $Pb_{50}Sn_{50}$ and the literature data [13]. As seen from the figure, the quantity D does not significantly depend on on the concentration. The mean square deviation of experimental points from the second-degree polynomial (it is not shown in the figure) which approximates the totality of data is equal to 12%. In out opinion, these differences do not exceed the errors of measurements inherent to the available methods to study the mutual diffusion. In particular, we did not observe any specific features of a behavior of the coefficient of mutual diffusion for a melt with the eutectic composition at least up to temperatures which are by 40 K higher the melting point for the eutectic (456 K).

The results of measurements of the electrical resistance are presented in Fig. 3. For all melts under study, the electrical resistance increases with the temperature almost linearly in the entire temperature interval. A good agreement between the curves of heating and cooling is traced. Melts were heated and cooled several times with different rates (200 and 100 K/h). Such

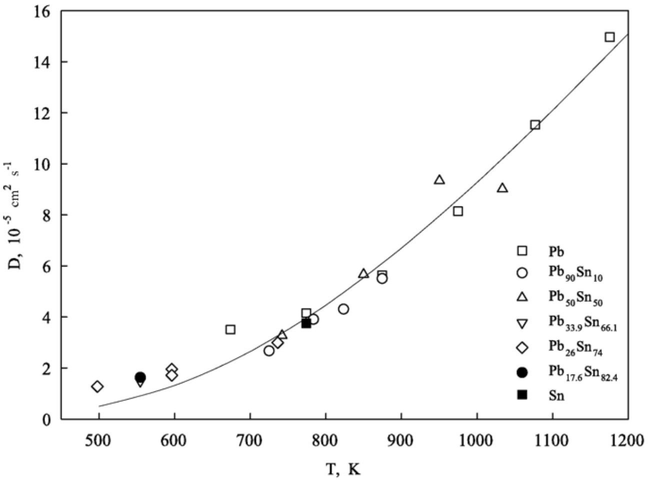

Fig. 2. Coefficients of mutual diffusion for melts of the Pb–Sn system. The continuous curve gives the approximation of data by the exponential function $D(T) = D_0 \exp(-E/RT)$ with the coefficients $D_0 = 1.73 \times 10^{-3}$ cm^{2}s^{-1}, $E = 24328$ J $\cdot$ mol^{-1}

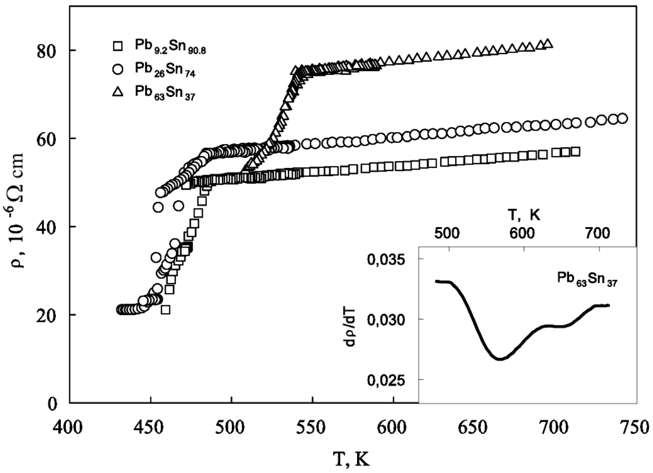

Fig. 3. Temperature dependence of the electrical resistance of melts of the Pb–Sn system

significant difference in the cooling rates has no considerable effect on the electrical resistance. The results obtained are in good agreement with data in [18–20]. In a narrow temperature interval between T_L and $T_L + 30$ K, where T_L is the liquidus temperature, the measurements were performed with a less rate of heating-cooling (20 K/h) and with a reduced step in the temperature (1–2 K). In this interval, the curve of the electrical resistance of the melt with $Pb_{9.2}Sn_{90.8}$ demonstrates the supercooling down to 470 K ($T_L = 484$ K), whereas no supercooling was revealed for the other compositions. On the curve $\rho(T)$ of the melt of $Pb_{26}Sn_{74}$, we observe a bend at a temperature of 484 K. The curves $\rho(T)$ for the melt of $Pb_{63}Sn_{37}$ show no similar hysteresis. The temperature dependence $S(T)$ is more complicated (Fig. 4). The absolute values of the thermopower at the cooling are higher than the corresponding values at the heating in all cases. The minimum of the eutectic concentration is caused by an insignificant effect of aftermelting. The crystallization of the melt of $Pb_{63}Sn_{37}$ occurs without anomalies. In Fig. 4, we present the temperature dependences of the thermopower, $S(T)$, which vary linearly with the temperature in the limits of experimental errors. The curves $S(T)$ for all compositions manifest the almost identical slope and have very small negative absolute values in the whole temperature range.

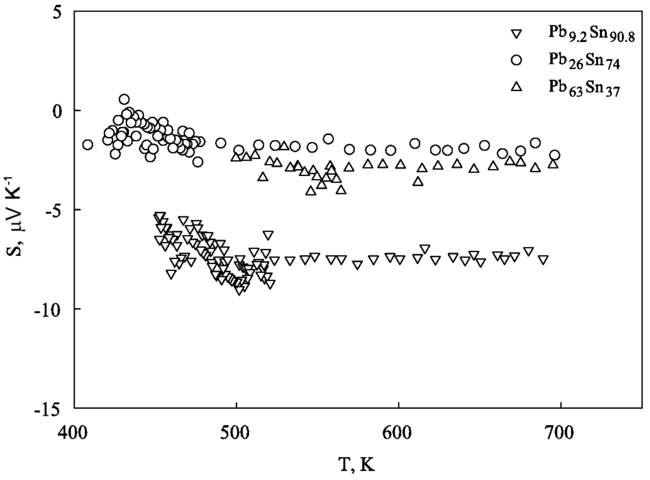

Fig. 4. Temperature dependence of the thermopower of melts of the Pb–Sn system

The temperature dependence of the heat conduction $\lambda(T)$ is studied in the temperature range between T_L and $T_L + 100$ K, where T_L is the liquidus temperature. The function $\lambda(T)$ is well described by the linear equation

$$\lambda = \lambda_0 + \frac{d\lambda}{dT}(T - T_{\mathrm{L}}), \qquad (2)$$

where $\lambda_0(T)$ is the heat conduction (in Wm^{-1} K^{-1}) at the melting point, and $\frac{d\lambda}{dT}$ is the temperature-dependent coefficient of heat conduction.

As seen from Fig. 5, the heat conduction of all melts under study increases in the course of heating by Eq. (2). Absolute values of the heat conduction, as well as its temperature dependence, testifies to the dominant contribution of the electron component of the heat transfer and to a rather strong degeneration of the electron gas

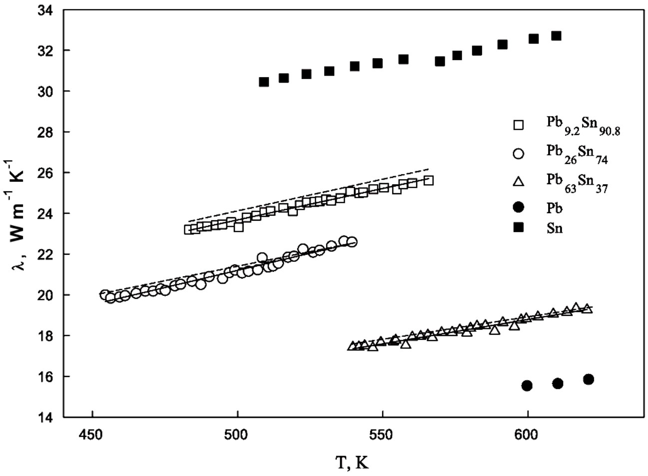

Fig. 5. Temperature dependence of the heat conduction of melts of the Pb–Sn system

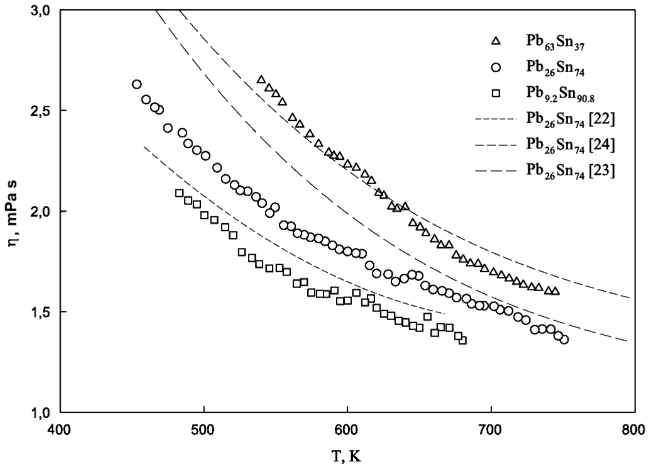

Fig. 6. Temperature dependence of the viscosity of melts of the Pb–Sn system

[21]. In this case, the Wiedemann–Franz–Lorentz law can be used, and the Lorentz number can be determined.

According to calculations, the Lorentz number is invariable in the temperature interval under consideration and is close to the theoretical value (Sommerfeld) 2.445×10^{-8} WK^{-2}. The experimental data on the heat conduction (continuous lines) are in good agreement with the data calculated by electrical conduction (dashed lines).

The results of studies of the viscosity are shown in Fig. 6 together with data of previous investigations for the eutectic composition [22–24]. In the process of cooling, the viscosity increases by the Arrhenius law. We note that, as distinct from the curves $\rho(T)$ and $S(T)$, the viscosity $\eta(T)$ has no anomalies in the whole range of temperatures.

4. Discussion of Results

Based on the results obtained, we may assume the formation of regions with the structures of tin and lead in the eutectic melt of $Pb_{26}Sn_{74}$. In other words, an eutectic mixture is formed. To confirm this assumption, we calculated the areas under the first maximum of the radial distribution curve and the position of the maximum, by assuming the existence of a quasieutectic structure and a structure with statistical distribution of atoms. In the first case, the formula for the area under the first maximum can be written as

$$Z = c_1 K_1^2 z_1(1) + c_2 K_2^2 z_2(2), \qquad (3)$$

where $K_1^2 = F_1^2/(c_1F_1^2+c_2F_2^2)$, $K_2^2 = F_2^2/(c_1F_1^2+c_2F_2^2)$, c_1, c_2, F_1, and F_2 are the concentrations and atomic scattering factors, respectively, of the first and second components, and $z_1(1)$ and $z_2(2)$ are the coordination numbers of the components. At $z_1(1)=10$ and $z_2(2)=8$, the calculated value $Z=9.0$ coincides practically with the experimental one equal to 8.3. In this case, the position of the first maximum determined from the relation $R_1 = c_1K_1^2R_1+c_2K_2^2R_2$ corresponds to 3.28 Å, which coincides practically with the experimental value of 3.3 Å. Hence, such structure model can be considered satisfactory. If we assume the statistical distribution of atoms, then the formula for the area under the first maximum takes the form

$$Z = (c_1K_1 + c_2K_2)^2(K_1z_1(1) + K_2z_2(2)), \qquad (4)$$

and the position of the first maximum $R_1 = (c_1K_1 + c_2K_2)^2(c_1R_1 + c_2R_2)$. In this case, $Z = 21.5$; $R_1 = 3.03$ Å, which disagrees with experimental data.

Therefore, we calculated the structural factor of the liquid eutectic $Pb_{26}Sn_{74}$ within the quasieutectic model. As seen from Fig. 1, the experimental and model structural factors are in good agreement.

The conclusion about a weak concentration dependence of the coefficient of mutual diffusion is confirmed by the analysis of thermodynamical characteristics of the liquid system Pb–Sn. It is known that the quantity D can be written as a product of the kinetic and thermodynamical factors

$$D = bC(1-C)(\partial^2 G/\partial C^2)_{P,T}, \qquad (5)$$

where b is the mobility, and G is the Gibbs free energy per mole of a solution. It was shown in [13] that the excessive volume of mixing is very small for Pb–Sn melts.

The excessive entropy of mixing is also equal to zero in the limits of the error of measurements, and the free energy of mixing $\Delta G(C)$ differs from $\Delta G_{\mathrm{id}}(C)$ for the ideal solution by at most 30%. Moreover, the experimental concentration dependence $\Delta G(C)$ is equal to $\Delta G_{\mathrm{id}}(C)$ multiplied by the constant in the limits of the error of data [13].

These facts allow us to state that the behavior of the liquid system Pb–Sn is in quite good agreement with the law of ideal solution, according to which $(\partial^2 G_{id}/\partial C^2)_{P,T} \approx 1/(C(1-C))$, and, respectively, the dependence $D(C)$ is determined by only the mobility [see formula (5). On the other hand, the mobility weakly depends on the composition, if the molar volumes of components of a melt are close. The molar volumes of liquid Pb and Sn differ only by 12% from each other, and, hence, the dependence $D(C)$ must be also weak, which is confirmed by experimental data.

The exponential dependence $D(T){=}D_0\exp(-E/RT)$, which is based on the assumption about the activation mechanism of the diffusion, describes satisfactorily the experimental data at temperatures higher than 600 K. However, at lower temperatures, the systematic deviations of experimental points from those given by the approximating equation are observed. The reason for the difference is possibly related to the assumption that the pre-exponential factor D_0 and the activation energy E were considered independent of the temperature.

Let us consider the dependence of electrical properties on the ordering of components of binary melts. According to the Matthiessen's rule, the specific electric resistance of a melt at the statistical distribution of impurity atoms

$$\rho_{\mathrm{st}} = \rho_0 + \Delta\rho \tag{6}$$

where ρ_0 is the resistance of the matrix, and $\Delta\rho$ is the additional resistance which is formed due to the presence of impurities. The appearance of an impurity in the matrix leads to changes in both the energy spectrum of carriers and the free path length. Therefore, relation (6) can be rewritten as

$$\rho_{\mathrm{st}} = \frac{12\pi\hbar}{S_{\mathrm{F}}^{\mathrm{st}} e^2 l_{\mathrm{st}}}, \tag{7}$$

where $S_{\mathrm{F}}^{\mathrm{st}}$ is the area of the Fermi surface of free electrons which is equal to $4\pi k^2$, $k = 2\pi(3N/4\pi)^{1/3}$, N is the number of atoms in unit volume, and l_{st} is the free path length.

The formation of microaggregates of atoms of a single sort is a fluctuating process by its character and cannot be accompanied by significant changes in the energy spectrum of electrons as compared with similar processes in a statistical melt. However, the character of the scattering must be changed due to a variation of the mobility of carriers. Let us assume that t be, according to the statistical distribution, a part of scvattering centers, and let $(1-t)$ be a part of atoms entering the microaggregates. Then the formula for the electrical resistance of a melt with similar distribution can be written as

$$\rho = \frac{12\pi\hbar^3}{S_{\mathrm{F}}^{\mathrm{st}} e^2} \frac{1}{[t l_{\mathrm{st}} + (1-t) l_{\mathrm{eut}}]}, \tag{8}$$

where l_{eut} is the free path length of electrons in microaggregates. It is known that the thermopower at high temperatures is mainly determined by its diffusion component [25]. Therefore, the thermopower of a metallic melt

$$S = -\frac{\pi^2\hbar^2 T}{3e}\left[\frac{d\ln(1/\rho)}{dE}\right]_{E=E_{\mathrm{F}}}. \tag{9}$$

We assume that the wave vector on the Fermi level is independent of the short-range order. Thus, the total thermopower

$$S = t\frac{\rho}{\rho^{\mathrm{st}}} S^{\mathrm{st}} + (1-t)\,\frac{\rho}{\rho^{\mathrm{eut}}} S^{\mathrm{eut}}, \tag{10}$$

where S^{st} is the thermopower of a statistically ordered melt, and S^{eut} is the thermopower corresponding to the eutectic ordering [see relation (9)].

We consider that these two types of a short-range order reflect, to a certain degree, a behavior of physical properties. By comparing the data obtained, we may assert that the majority of specific features is revealed in melts with a higher content of tin, whereas they are less pronounced, for example, for $\mathrm{Pb_{63}Sn_{37}}$. The behavior of $S(T)$ admits the existence of a metastable nonequilibrium quasieutectic structure in the melt. Insignificant admixtures of tin are dissolved at their introduction into a loose package of liquid lead, make a short-range order of the matrix more compact, and regulate the ordering of scattering centers. These centers are a reason for an increase in the mobility of carriers and, hence, for an increase in the electrical conduction at the transition from pure Pb to pure Sn.

According to the model proposed in [2], eutectic systems in the liquid state contain regions with different thermodynamical stabilities. Like the systems with stratification, such regions are separated by lines of the spinodal, S, and the binodal, B. However, no typical separation of phases in a clearly expressed form is observed in this case. These regions manifest themselves as anomalous fluctuations of the concentration, which is

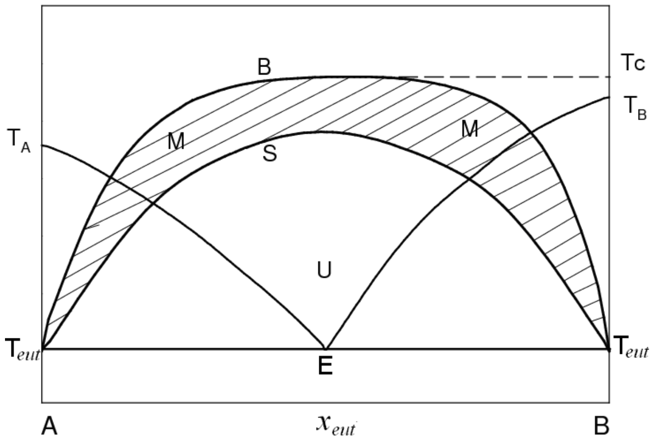

Fig. 7. Regions with different thermodynamical stabilities in eutectic systems. U – unstable state, M – metastable state, B – binodal line, S – spinodal line, T_AET_B – liquidus line, $T_{\text{eut}}ET_{\text{eut}}$ – solidus line, and x_{eut} – eutectic concentration

reflected, in turn, in a change of the generally foreseen physical properties. The observed phenomenon can be considered as a certain type of the microsegregation.

The systems with stratification were studied in a number of previous works [26–29]. The proposed theoretical method is related to the use of a microscopic approach of the phase transition of stratification in a model of binary symmetric mixture. With the development of theoretical schemes used in the description of phase transitions [30] in the presence of an external field, we get a possibility to describe the phase transition of stratification in any (not only symmetric) model of mixture. The importance of such an approach consists in the possibility to study the influence of microscopic parameters of a system, particularly the interaction potential, on the critical behavior.

After the melting, the quasieutectic structure of a chemically heterogeneous melt retains, and the concentration gradient is formed over the height. It is assumed that reversible variations in the composition of a melt and in the size of particles occur in a temperature interval with the linear dependence $\rho(T)$ (the slope $\frac{d\rho}{dT}$ is almost constant). The particles are in a metastable equilibrium with the matrix. After the attainment of a temperature which is characteristic of each composition and is distinguished by a bend on the curve $\rho(T)$ or by a sharp change in $\frac{d\rho}{dT}$, the dissolution of particles starts. Since the intersurface tension decelerates this process, a microinhomogeneous melt can retain even at quite high temperatures.

It was proposed [2] to determine the boundaries of the microinhomogeneous stability of eutectic melts by the extrapolation of the curves of bounded solubility in the solid state to a region above the liquidus. Thus method is based on the ideas developed earlier by Frenkel [31]. According to [2], the spinodal, as the limiting line of stability of a homogeneous melt, has a maximum, whose position cannot exceed $2T_{\text{eut}}$, where T_{eut} is the temperature of the eutectic. The results of our work do not confirm that assertion. The absence of bends on the curves $\rho(T)$ and a weak temperature dependence of $\frac{d\rho}{dT}$ foresee higher characteristic values than $2T_{\text{eut}}$ for each system.

For example, the value of $2T_{\text{eut}}$ for the eutectic $\text{Pb}_{26}\text{Sn}_{74}$ is near 916 K. But, by our experimental data, the transition to the stable state occurs at 1350 K in $\text{Pb}_{26}\text{Sn}_{74}$. In other words, the line of the binodal B is the boundary of a region with a metastable, M, quasieutectic structure of the melt, rather than an unstable, U, one (Fig. 7). This line is positioned significantly above the lines of bounded solubility extrapolated into the liquid phase. It is possible that the lower points of the binodal coincide with points of the intersection of these curves with a horizontal of the eutectic. In practice, a very fast passage of the temperature interval between the curve of bounded solubility and the liquidus prevent a homogenization of the solid phase.

As a result, the inhomogeneities will be conserved in a melt. The further heating leads to the equating of compositions of particles and the surrounding melt. in the highest point of the binodal, these compositions coincide, and the metastable state of a microemulsion cannot be realized further. We consider, however, that such a metastable state can retain for a long term under nonequilibrium conditions also at higher temperatures.

5. Conclusions

The revealed specific features of behavior of the coefficient of mutual diffusion in melts of the Pb–Sn system at temperatures lower than 600 K, as well as the observed hysteresis-like distinctions between the heating-cooling curves for temperature dependences of some electrophysical and structure-sensitive properties, can be related to the existence of a metastable microheterogeneous structure of a melt.

The present work is partially supported by the State Fund of Fundamental Research (SFFR) (Ukrainian-Russian project F28-255/2009).

1. K. Bae, A.F. Sprecher, H. Conrad, and D.Y. Jung, in: *International Symp. Testing and Failure Analysis* (ASM Int., Materials Park, OH, 1988), p. 53.

2. E.V. Kalashnikov, Technical Physics **67**, 330 (1997).
3. W.B. Castro, M. Lucena Maia, C.S. Kiminami, and C. Bofarini, Mater. Sci. Eng. A. **304-306**, 255 (2001).
4. C. Frueh, D.R. Poirier, and S.D. Felicelli, Mater. Sci. Eng. A. **328**, 245 (2002).
5. O.L. Rocha, C.A. Siqueira, and A. Garcia, Mater. Sci. Eng. A. **59**, 347 (2003).
6. P.S. Popel', E.L. Presnyakova, V.A. Pavlov, and E.L. Arkhangel'skii, Metally **2**, 53 (1985).
7. U. Dahlborg, M. Calvo-Dahlborg, P. Popel, and V. Sidorov, Eur. Phys. J. **B14**, 639 (2000).
8. P.S. Popel', E.L. Presnyakova, V.A. Pavlov, and E.L. Arkhangel'skii, Metally **4**, 198 (1985).
9. F.Q. Zu, Z.G. Zhu, B. Zhang, Y. Feng, J.P. Shui, J. Phys.: Condens. Matter **13**, 1145 (2001).
10. C.A. Siqueira, N. Cheung, and A. Garcia, J. Alloys Comp. **351**, 126 (2003).
11. A.P. Belaev, S.A. Kukushkin, and V.P. Rubets, Physics of the Solid State **43**, 597 (2001).
12. D.T. Cromer and J.T. Waber, Acta Cryst. **18**, 104 (1965).
13. R.A. Khairulin, S.V. Stankus, and P.P. Bezverkhy, J. Alloys Compd. **312**, 211 (2000).
14. Yu. Plevachuk and V. Sklyarchuk, Meas. Sci. Technol. **12**, 23 (2001).
15. V. Sklyarchuk and Yu. Plevachuk, Meas. Sci. Technol. **16**, 467 (2005).
16. S. Mudry, V. Sklyarchuk, and A. Yakymovych, J. Phys. Studies. **12**, 1601 (2008).
17. J. Vollmann, F. Herwig, and M. Wobst, Exp. Techn. Phys. **39**, 527 (1991).
18. Y. Plevachuk, V. Sklyarchuk, A. Yakymovych, B. Willers, and S. Eckert, J. Alloys Compd. **394**, 63 (2005).
19. A. Roll and G. Fees, Z. Metallkd. **51**, 540 (1960).
20. P.D. Adams, Phys. Rev. **156**, 178 (1967).
21. J.M. Ziman, *The Physics of Metals*, (Cambridge University Press, Cambridge, 1969), Chapters 5 and 6.
22. H.J. Fischer and A. Phillips, J. of Metals **9**, 1060 (1954).
23. E. Gebhardt and K. Kostlin, Z. Metallkd. **48**, 636 (1957).
24. F. Herwig and M. Wobst, Wiss. Z. der TU Chemnitz **4**, 391 (1991).
25. N.F. Mott and E. Davis, *Electron Processes in Non-Crystalline Materials* (Clarendon Press, Oxford, 1979).
26. M.P. Kozlovskii, O.V. Patsahan, and R.S. Melnyk, Ukr. Fiz. Zh. **45**, 381 (2000).
27. O.V. Patsahan and M.P. Kozlovskii, Condens. Matter Phys. **45**, 607 (2000).
28. O.V. Patsahan, M.P. Kozlovskii, and R.S. Melnyk, Condens. Matter Phys. **12**, 1595 (2000).
29. O.V. Patsahan, M.P. Kozlovskii, and R.S. Melnyk, Condens. Matter Phys. **4**, 235 (2001).
30. M.P. Kozlovskii, Ukr. Fiz. Zh. **5**, 61 (2009).
31. J. Frenkel, *Kinetic Theory of Liquids* (Clarendon Press, Oxford, 1946).

Received 07.03.10.
Translated from Ukrainian by V.V. Kukhtin

СТРУКТУРА ТА ФІЗИЧНІ ВЛАСТИВОСТІ РОЗПЛАВІВ Pb–Sn

В. Склярчук, А. Якимович, І. Штаблавий, І. Шевернога, М. Козловський, Р. Хайрулін, С. Станкус

Резюме

Структура, взаємна дифузія, електроопір, термо-ерс та в'язкість розплавів Pb–Sn досліджені в широкому температурному інтервалі. На базі виявлених розбіжностей між кривими нагріву та охолодження температурних залежностей електрофізичних і структурно-чутливих властивостей, а також гістерезису в циклах нагріву–охолодження, припускається існування в розплавах Pb–Sn метастабільної мікрогетерогенної структури в певному температурному інтервалі.